Inorganic Chemistry

Article

pubs.acs.org/IC

Heterometallic Second-Row Transition Metal Chain Compounds in Two Charge States: Syntheses, Properties, and Electronic Structures of [Mo−Mo−Ru]$^{6+/7+}$ Chains

David W. Brogden and John F. Berry*

Department of Chemistry, University of Wisconsin—Madison, 1101 University Avenue, Madison, Wisconsin 53706, United States

Supporting Information

ABSTRACT: Reaction of $Mo_2(dpa)_4$ (dpa = 2,2′-dipyridylamido) with $^1/_2$ equiv of $[Ru(CO)_3Cl_2]_2$ in molten naphthalene at 250 °C provides facile access to the first all-second-row transition metal heterometallic chain compound, MoMoRu-$(dpa)_4Cl_2$ (**1**). The one-electron oxidized compound $[MoMoRu(dpa)_4Cl_2](OTf)$ (**2**) is synthesized by reaction of **1** with $FeCp_2(OTf)$. X-ray crystallography reveals a contraction of the Mo−Ru bond distance from 2.38 Å in **1** to 2.30 Å in **2**, and an elongation of the Mo−Mo bond distance from 2.12 Å in **1** to 2.21 Å in **2**. The short Mo−Ru bond distances indicate significant electron delocalization along the Mo−Mo−Ru chain, which is quantified by density functional theory (DFT) calculations. Molecular orbital analyses of both compounds based on DFT results reveal full delocalization of the orbitals of σ and π symmetry for both compounds. Additionally, δ orbital delocalization is observed in **2**.

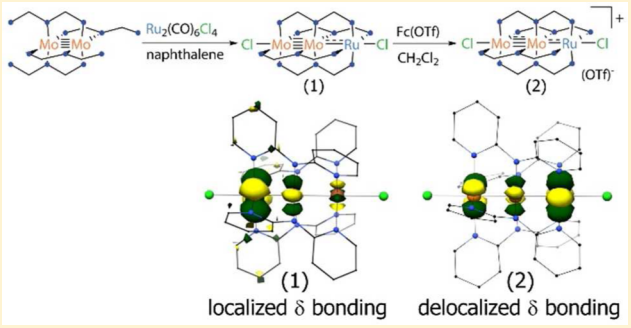

INTRODUCTION

Recently, the chemistry of mixed-metal heterometallic compounds has undergone a renaissance,[1−6] and one area of significant interest is in the preparation and properties of heterometallic compounds containing a linear chain of transition metals.[7,8] Of these, heterometallic trinuclear chain compounds supported by the 2,2′-dipyridylamido ligand (dpa) are the simplest, and three separate classes of these have been prepared. Symmetric $M_A-M_B-M_A$ compounds are typically prepared via high-temperature self-assembly methods and feature a d^8, square-planar transition metal in site B (Ni, Pd, or Pt), with other first-row metals employed in sites A.[8] Heterotrimetallic $M_A-M_B-M_C$ compounds with three different metals are difficult to prepare, but may be made taking advantage of heterobimetallic starting materials[9] or by metal atom substitution using labile first-row metals.[10] The most numerous class of trinuclear heterometallic chains are those with a $M_A-M_A-M_B$ core, for which we have developed a rational, stepwise synthetic approach based on the addition of a mononuclear M_B starting material to a preformed bimetallic M_A-M_A complex.[11−14] Until recently, all of these synthetic methods have required the use of at least one first-row transition metal.

A further limitation of the chemistry of the above-mentioned chain compounds is that many are unstable to further chemical transformations. For example, we have found ligand substitution reactions of $M_A-M_A-M_B$ compounds to be difficult, often due to demetalation and loss of M_B.[15,16] Also, although we have extensively investigated electrochemical features of the trinuclear heterometallic compounds,[14] to date no heterometallic $M_A-M_A-M_B$ chain compound has proven stable enough to yield an isostructural oxidation or reduction product.[17] Chemical oxidation of $CrCrFe(dpa)_4Cl_2$ was attempted, but the product was only fleetingly stable and could only be characterized by a low-temperature EPR spectrum.[11]

We recently communicated our results on the first trinuclear all second-row heterometallic chain compound, MoMoRu-$(dpa)_4Cl_2$ (**1**).[18] Compound **1** has proven stable enough that its unprecedented monocation $[MoMoRu(dpa)_4Cl_2]^+$ (**2**) can be prepared. In this work, we compare the properties of the MoMoRu chain in two oxidation states to gain insights into the charge distribution throughout the compounds.

RESULTS AND DISCUSSION

Synthesis. Creating linear chain compounds using second-row transition metals is a major challenge since these metals are more kinetically inert than their first-row transition metal counterparts. For example, the homometallic $M_3(dpa)_4Cl_2$ compounds with first-row metals are easily prepared in high yields in refluxing THF,[19] but the second-row analogues $Ru_3(dpa)_4Cl_2$ and $Rh_3(dpa)_4Cl_2$ were originally reported in very low yields,[20] which have been recently improved significantly.[21,22] Due to the kinetic inertness of these metals, very high temperatures are required to prepare them, and

Received: June 18, 2015
Published: July 22, 2015

DOI: 10.1021/acs.inorgchem.5b01370
Inorg. Chem. 2015, 54, 7660−7665

molten naphthalene is so far the only solvent that has been used to successfully prepare these compounds.[21−23]

The other synthetic difficulty with second-row transition metals is the fact that analogues of the simple MCl_2 salts that have proven highly successful in first-row transition metal chemistry are simply unavailable. For Ru, synthetically useful ligated $RuCl_2$ adducts such as $RuCl_2(DMSO)_4$ and $Ru_2(benzene)_2Cl_4$ are known and were tested, but even in molten naphthalene, loss of the supporting ligands is problematic. Noting that metal carbonyl complexes had been successfully used as precursors to dpa complexes in naphthalene,[24] we attempted the preparation of $MoMoRu(dpa)_4Cl_2$, **1**, by reaction of $Mo_2(dpa)_4$ with $^1/_2$ equiv of $[Ru(CO)_3Cl_2]_2$ at 250 °C. Over the course of 12 h the red $Mo_2(dpa)_4$ solid changes to brown to signal that the reaction is complete. Compound **1** is easily isolated following the removal of naphthalene, extraction with dichloromethane, and crystallization from dichloromethane/hexanes.[18]

The observation of a reversible wave in the cyclic voltammogram (CV) of **1** at −0.54 V versus Fc/Fc^+ suggested that a one-electron oxidized compound might be stable.[18] An oxidized compound would be valuable to help further our understanding of the electronic structure of second-row M_A−M_A−M_B chains. As mentioned above, however, previous attempts to isolate a one-electron oxidized product of the similar first-row compound, $Cr_2Fe(dpa)_4Cl_2$, were unsuccessful due to the chemical instability of the oxidized complex. We nevertheless attempted chemical one-electron oxidation of **1** by reaction with the mild oxidizing agent $FeCp_2(OTf)$. Upon the addition of 1 equiv of $FeCp_2(OTf)$ in dichloromethane, Scheme 1, the brown solution of **1** turned to purple. After

Scheme 1. Synthetic Routes to First-Row Heterometallic Chains (Top), 1 (Middle), and 2 (Bottom)

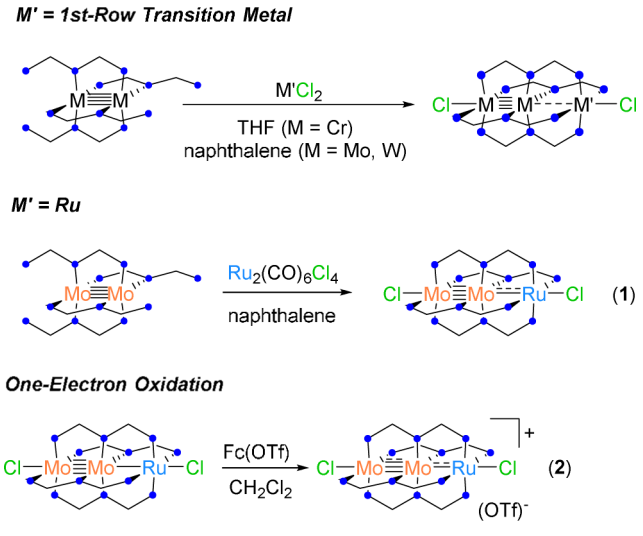

removal of the solvent and washing the resulting solid with diethyl ether to remove the reduced $FeCp_2$, the oxidized compound $[MoMoRu(dpa)_4Cl_2](OTf)$, **2**, could be recrystallized by slow diffusion of either hexane or diethyl ether into a dichloromethane solution of **2**. A unique property of **2** that has not been observed before for other heterometallic chain compounds is that it is air-stable in solution for a period of days and indefinitely in the solid form.

Crystal Structures. Compounds **1** and **2** have both been examined by X-ray crystallography. Whereas the asymmetric unit of **1** contains two independent $MoMoRu(dpa)_4Cl_2$ units, with minor metal atom disorder along the heterometallic Mo—Mo—Ru chain, and two dichloromethane solvent molecules, the asymmetric unit of **2** contains only one heterometallic Mo—Mo—Ru chain, without any metal atom disorder, supported by four equatorial dpa ligands, with two axial Cl^- ions. Additionally, **2** has an outer-sphere triflate ion in the structure, indicating the cationic nature of the $[MoMoRu(dpa)_4Cl_2]^+$ core. Interestingly, the asymmetric unit of **2** is devoid of any solvent molecules, which allows the molecule to crystallize with the same unit cell from either dichloromethane/hexane or dichloromethane/diethyl ether solvent combinations. The crystal structure of **2** is shown in Figure 1, and the crystal

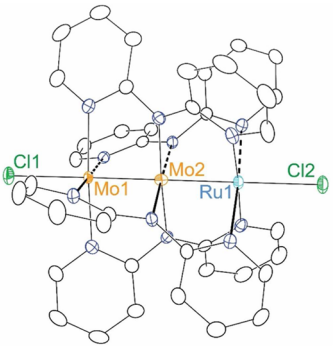

Figure 1. X-ray crystal structure of **2**, with thermal ellipsoids drawn at the 50% probability level. Hydrogen atoms and the triflate counteranion have been omitted for clarity.

structure of **1** is shown in the Supporting Information Figure S1. The Mo—Mo distance in **1**, 2.12 Å, is slightly longer than the Mo≡Mo bond distance in the $Mo_2(dpa)_4$ starting material, 2.10 Å (Table 1). Upon oxidation, however, the Mo—Mo distance increases significantly to 2.21 Å. As compared to the oxidative elongation of the Mo≡Mo bond by 0.03 Å in $[Mo_2(dpa)_4]^{0/+}$,[24] the elongation of this bond by ∼0.09 Å going from **1** to **2** signifies that there is more going on in this oxidation than simply the removal of a Mo≡Mo δ electron. By means of comparison, the typical elongation of a Mo≡Mo bond by removal of a δ electron is in the range 0.04−0.06 Å.[25−29]

The other important piece of the puzzle is the heterometallic Mo−Ru distance, which shortens from an already remarkably short distance of 2.38 to 2.30 Å upon oxidation of **1** to **2**. These changes suggest that Mo−Ru bonding is increased in **2** at the expense of some Mo−Mo bonding character. Another further factor that likely influences the Mo−Mo bond length is the fact that the axial Mo−Cl distance shrinks from 2.53 to 2.46 Å upon oxidation of **1** to **2**. The Ru−Cl distance also shortens upon oxidation, but only by ∼0.04 Å.

Solution Properties. The electronic absorption spectrum of **2** collected in dichloromethane at room temperature is shown in Figure 2 and compared to the spectrum of **1**. Both spectra display rich absorption features in the visible region. Compound **1** is characterized by four features at <400, 505, 630, and 730 nm. Compound **2** displays four absorption features at <400, 445, 535, and 960 nm. The lowest energy feature of **1**, at 730 nm, was previously attributed to the Mo_2 $\delta \rightarrow \delta^*$ transition, whereas the higher energy features, < 700 nm, were described as charge-transfer transitions.[18] However, due to

DOI: 10.1021/acs.inorgchem.5b01370
Inorg. Chem. 2015, 54, 7660−7665

Table 1. Experimental and Calculated Bond Distances (Å) for 1 and 2

compd	Mo−Mo	Mo−Ru	Mo−Cl	Ru−Cl	Mo−N_{py}	Mo−N_a	Ru−N_{py}
$Mo_2Ru(dpa)_4Cl_2$ (**1**)	2.1229[4]	2.3841[5]	2.5311[7]	2.4941[7]	2.185[2]	2.110[2]	2.092[2]
$Mo_2Ru(dpa)_4Cl_2$ (**1**) DFT	2.146	2.395	2.525	2.525	2.208	2.135	2.107
$Mo_2Ru(dpa)_4Cl_2(OTf)$ (**2**)	2.2130(3)	2.3010(2)	2.4637(5)	2.4586(5)	2.176[2]	2.088[2]	2.121[2]
$Mo_2Ru(dpa)_4Cl_2(OTf)$ (**2**) DFT	2.191	2.362	2.478	2.478	2.217	2.119	2.114

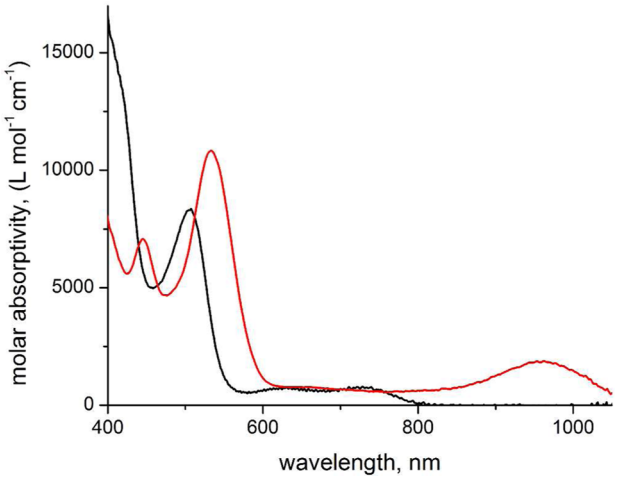

Figure 2. Electronic absorption spectrum of $Mo_2Ru(dpa)_4Cl_2$ (**1** black)[18] and $[Mo_2Ru(dpa)_4Cl_2](OTf)$ (**2** red) in CH_2Cl_2 measured at room temperature.

the oxidation of **1** the HOMO and LUMO of **2** are no longer the δ and δ^* orbitals (vide infra); therefore, the nature of the absorption feature at 960 nm is tentatively assigned as a metal-to-metal charge-transfer band. The higher energy features in **2** are most likely charge-transfer bands due to their intensity, $\varepsilon >$ 6000 L mol^{-1} cm^{-1}.

Compound **1** was previously shown to be diamagnetic by NMR spectroscopy;[18] therefore, the one-electron oxidized compound **2** should be paramagnetic. To characterize the paramagnetic nature of **2**, X-band EPR data were collected at 8 K, Figure 3. Compound **2** displays an axial signal with broad features and visible satellite shoulders indicating hyperfine interactions. The spectrum is best simulated by modeling the

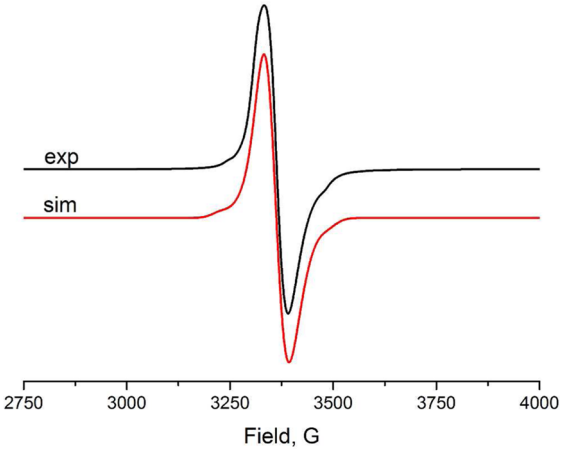

Figure 3. EPR data and simulation for $[Mo_2Ru(dpa)_4Cl_2]^+$ (**2**) at 8 K. Simulation parameters are as follows: freq = 9.380 GHz; $g_\parallel$ = 1.997, $g_\perp$ = 1.989; $A_\parallel$ = 135 MHz, $A_\perp$ = 55 MHz; HStrain = (120, 245, 245); lw = 2; points = 4096.

unpaired electron to be localized on one Mo center, justified by the results of the DFT spin density analysis (vide infra), which show the unpaired electron to be localized on the outer Mo atom. The simulation parameters are $g_\parallel$ = 1.997 and $g_\perp$ = 1.989, and the corresponding A values are $A_\parallel$ = 135 MHz and $A_\perp$ = 55 MHz. Because the unpaired electron is localized on one of the Mo atoms, it is apt to compare the g and A values to other Mo_2 and heterometallic MoW compounds. The oxidized homo-bimetallic compounds $[Mo_2(dpa)_4]^+$, $[Mo_2(O_2C^tBu)_4]^+$, $[Mo_2(TiPB)_4]^+$ (TiPB = 2,4,6-triisopropylphenyl carboxylate), and $[Mo_2(O_2CC_3H_7)_4]^+$ along with the heterometallic $[MoW(O_2C^tBu)_4]^+$ and $[MoW(dpa)_4]^+$ have all been characterized by EPR spectroscopy.[18,24,27,28,30] For the $[Mo_2(dpa)_4]^+$ and $[Mo_2(O_2C^tBu)_4]^+$ compounds, the EPR spectra display isotropic signals, g = 1.951 (A = 57 MHz)[24] and g = 1.941 (A = 27 MHz),[28] respectively. The compounds $[Mo_2(TiPB)_4]^+$ and $[Mo_2(O_2CC_3H_7)_4]^+$ display isotropic g values, g = 1.951 and g = 1.941, respectively; however, these compounds display axial A values, $A_\parallel$ = 107 MHz and $A_\perp$ = 55 MHz[27] for $[Mo_2(TiPB)_4]^+$ and $A_\parallel$ = 107 MHz and $A_\perp$ = 53 MHz[30] for $[Mo_2(O_2CC_3H_7)_4]^+$. The g values of **2** are slightly larger than those displayed by the bimetallic Mo_2 compounds, but they are less than the free electron g value as expected for a Mo-based system. The observed A values for **2** are larger than those in the Mo_2 compounds, in agreement with the greater localization of the unpaired electron on only one Mo atom. Like the Mo_2^{5+} compounds, **2** displays a larger $A_\parallel$ value than $A_\perp$. The heterometallic compounds, $[MoW(O_2C^tBu)_4]^+$ and $[MoW(dpa)_4]^+$, are also worth including in this comparison because their spin density is polarized toward the Mo atom by ~70:30. Both compounds display isotropic g values, g = 1.881 and g = 1.908, respectively, and have corresponding A values that are larger for Mo than W: $A_{iso,Mo}$ = 115 MHz and $A_{iso,W}$ = 78 MHz[28] for $[MoW(O_2C^tBu)_4]^+$ and $A_{iso,Mo}$ = 80 MHz and $A_{iso,W}$ = 70 MHz[18] for $[MoW(dpa)_4]^+$. Clearly, the nature of the equatorial ligand (O,O vs N,N donors) has a major influence on A_{iso}. The A_{iso} value of **2** ($A_{iso} = (A_\parallel + 2A_\perp)/3$) of 82 MHz matches well that of the latter compound.

Electronic Structures. Density functional theory (DFT) calculations on closed shell compound **1** reveal significant σ and π electron delocalization along the Mo−Mo−Ru chain, resulting in a 3-center/2-electron (3c/2e) σ bond and two 3c/4e π bonds. While the σ and π orbitals in **1** are delocalized, the δ orbitals are localized on the Mo atoms with very little Ru character (<10%). Thus, the highest occupied and lowest unoccupied molecular orbitals of **1** are the Mo_2 δ and δ^* orbitals, Figure 4; a simple Koopmans' theorem prediction would therefore be that a Mo−Mo δ electron should be lost upon oxidation. In this case, the oxidation should be mostly localized on the Mo_2 unit, and would be expected to affect the Mo−Mo bond distance and little else. Clearly, from the geometric features of **2** detailed above, this simple picture is not adequate.

Thus, DFT calculations were performed on **2** to further investigate its electronic structure. The DFT optimized

DOI: 10.1021/acs.inorgchem.5b01370
Inorg. Chem. 2015, 54, 7660−7665

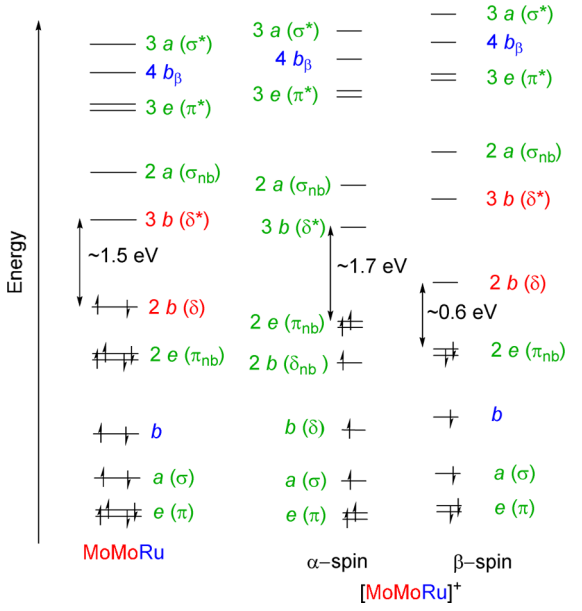

Figure 4. (Left) Comparison of molecular orbital diagrams for **1** (left) and **2** (right). Orbitals localized on the Mo_2 unit are given with red labels, blue labels represent Ru-centered orbitals, and the green labels indicate orbitals that show significant delocalization throughout the Mo−Mo−Ru chain.

structure of **2**, Table 1, slightly underestimates the Mo−Mo bond distance at 2.19 Å and overestimates the Mo−Ru distance at 2.36 Å. Nevertheless, the calculations do predict correctly the observed elongation of the Mo−Mo bond and contraction of the Mo−Ru bond upon removal of an electron from **1**. The calculated M−Cl and M−N distances correspond well to the experimental values.

The DFT predicted α and β molecular orbitals of **2**, depicted in Figure 5 and Supporting Information Figures S2 and S3, show very different features. The β orbitals display the same ordering as that observed for **1**, with the LUMO now being the localized Mo−Mo δ orbital (b symmetry in the C_4 point group), and the degenerate delocalized π_{nb} orbitals (e symmetry) as the HOMOs, Figure 4. The β set shows an

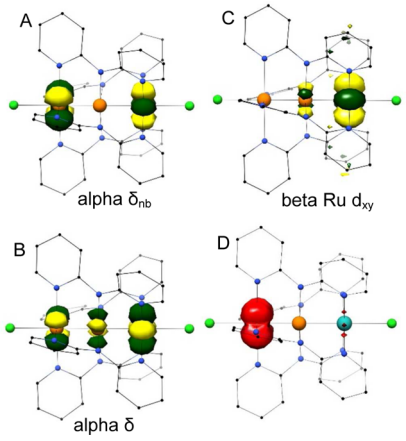

Figure 5. (A) $2b$ (δ_{nb}) α molecular orbital for **2**. (B) b (δ) α molecular orbital for **2**. (C) b (Ru d_{xy}) β molecular orbital for **2**. (D) Spin density plot for **2** emphasizing the location of the unpaired electron density on the outer Mo atom. Orange spheres represent Mo, and the teal sphere represents Ru.

approximately localized set of δ-symmetry orbitals: the Mo_2 δ and δ^* orbitals $2b$ and $3b$, both having only 9% Ru character, and a Ru-based d_{xy} orbital, $1b$, with only 11% Mo character.

The α molecular orbitals display a very different ordering compared to the β set, and are significantly more delocalized. In addition to delocalized σ (a symmetry) and π orbitals, there are also now delocalized δ orbitals. The δ bonding combination, for example, has contributions from both Mo atoms (summing to 45%) and the Ru atom (55%). The δ nonbonding orbital, as expected from classic molecular orbital theory, has a node at the central Mo atom, but nearly equivalent character at the outer Mo and Ru atoms of 60% and 40%, respectively. The δ bonding and nonbonding orbitals each house an α-spin electron, and thus, the compound may be considered to have a 3c/2e Mo−Mo−Ru δ bonding interaction, in addition to the 3-center σ and π interactions that are already present. The α orbitals thus display a completely delocalized bonding network, similar to that predicted for symmetric homometallic chain compounds.[8,21,31]

Since the α-spin δ and δ_{nb} electrons are delocalized throughout the Mo−Mo−Ru chain and the β-spin δ-symmetry electron is in a Ru-based localized orbital, the spin density of **2** is significantly localized on the outer Mo atom. The predicted spin populations for Mo1, Mo2, and Ru are 0.89, −0.04, 0.02, respectively, Figure 5.

The effect of the one-electron oxidation on the metal−metal bonding along the Mo−Mo−Ru chain may also be analyzed by the calculated Mayer bond order (MBO) values, Table 2. The

Table 2. Calculated Mayer Bond Orders for 1 and 2

compd	Mo−Mo	Mo_{inner}−Ru	Mo_{outer}−Ru
$Mo_2Ru(dpa)_4Cl_2$ (**1**)	2.49	1.12	0.36
$(Mo_2Ru(dpa)_4Cl_2)(OTf)$ (**2**)	2.30	1.23	0.39

decrease of the Mo−Mo MBO from 2.49 for **1** to 2.20 for **2** is indicative of weakening the Mo−Mo bond, and the slight increase of both the Mo−Ru_{inner} and Mo−Ru_{outer} MBO values to 1.23 and 0.39, respectively, supports the greater amount of electron delocalization in **2** as compared to **1**.

The electronic absorption spectrum of **2**, Figure 2, showcases rich absorption features at 965, 535, 445, and <400 nm. The lowest energy absorption features in compounds such as **1** and the analogous $Mo_2Fe(dpa)_4Cl_2$ compound have been assigned as Mo_2 $\delta \rightarrow \delta^*$ transitions.[14] In this case, however, due to the loss of a δ electron, time-dependent DFT (TD-DFT) calculations performed on **2** predict the lowest energy feature to be a mix of Ru-to-Mo and ligand-to-metal charge transfer. The higher energy absorptions are predicted to be charge-transfer bands in agreement with similar observations for **1**.

Summary. We have described a synthetic strategy for the preparation of Mo−Mo−Ru chain compounds in two different oxidation states. In a comparison of the $[MoMoRu]^{6+/7+}$ compounds, the oxidized product displays a shorter Mo−Ru distance, leading to significantly more electron delocalization along the Mo−Mo−Ru chain than in **1**. The β molecular orbitals display delocalized σ and π orbitals, whereas the α molecular orbitals show complete σ, π, and δ delocalization. Although Mo−Ru δ bonding has been contemplated in previously reported Mo−Ru bimetallic compounds,[32,33] to our knowledge **2** is the first compound yet reported for which DFT calculations indicate delocalized Mo−Ru δ bonding.

DOI: 10.1021/acs.inorgchem.5b01370
Inorg. Chem. 2015, 54, 7660−7665

EXPERIMENTAL SECTION

Materials and Methods. All reactions were carried out under a dry N_2 atmosphere using Schlenk techniques and glovebox methods. Hexane and diethyl either were purified using a Vacuum Atmospheres solvent purification system, and dichloromethane was freshly distilled under a N_2 atmosphere over CaH_2 prior to use. $FeCp_2(OTf)$[34] and $Mo_2(dpa)_4$[18] were prepared according to literature procedures. Naphthalene was purchased from Sigma-Aldrich and sublimed prior to use. $[Ru(CO)_3Cl_2]_2$ was purchased from Strem Chemicals and used as received. Elemental analysis was carried out by Midwest Microlab, LLC, Indianapolis, IN. IR spectra were taken on a BRUKER TENSOR 27 FTIR spectrometer using an attenuated total reflectance (ATR) adapter. The EPR measurement was carried out at 8 K using a Bruker EleXsys EPR spectrometer (E-500-A console with ER 049SX SuperX bridge and SuperX cavity). The parameters were as follows: frequency = 9.380 GHz, microwave power = 0.6325 mW, field center = 3390 G, field width = 2000 G, modulation amplitude = 4 G, modulation frequency = 100 kHz, time constant = 163.84 ms.

Crystallography. Crystallographic data were measured at the Molecular Structure Laboratory of the Chemistry Department of the University of Wisconsin—Madison. Crystals were selected under oil under ambient conditions and attached to the tip of a MiTeGen MicroMount. Each crystal was mounted in a stream of cold nitrogen at 100(1) K and centered in the X-ray beam using a video camera. The crystal evaluation and data collection were performed on a Bruker Quazar SMART APEXII diffractometer with Mo Kα (λ = 0.710 73 Å) radiation with the detector to crystal distance of 5.0 cm. The data were collected using a routine to survey an entire sphere of reciprocal space, and were indexed by the SMART program.[35] The structures were solved using direct methods and refined by least-squares refinement on F^2 followed by difference Fourier synthesis.[36] All hydrogen atoms were included in the final structure factor calculation at idealized positions and were allowed to ride on the neighboring atoms with relative isotropic displacement coefficients.

Computational Methods. Calculations were performed using ORCA version 2.9.1.[37] The initial coordinates for the calculations were obtained from the crystallographic data for **1** and **2**. The BP86 functional[38,39] and the RI/J approximation[40] were used for all calculations. Geometry optimizations of **1** and **2** were performed with the def2-SV(P) basis set[41] and def2-SVP/J auxiliary basis set[42,43] for C and H atoms, def2-TZVP(-f) basis set[44] and def2-TZVP/J auxiliary basis set[42,43] for N and Cl atoms, and the def2-TZVPP basis set[44] and def2-TZVPP/J auxiliary basis set[42,43] for Mo and Ru atoms including the ZORA approximation.[45] Tight optimization and tight self-consistent field convergence were employed along with grid5 for all geometry optimization calculations. Löwdin population analysis was used to determine orbital populations.[46−48] Orbital analysis and molecular graphics were performed with the UCSF Chimera package.[49] All DFT calculations were performed on unconstrained structures. Symmetry labels presented in the molecular orbitals diagrams were assigned by inspection to conform to the idealized C_4 point group.

*$MoMoRu(dpa)_4Cl_2$ (**1**).* Solid red $Mo_2(dpa)_4$ (0.299 g, 0.343 mmol) and $[Ru(CO)_3Cl_2]_2$ (98.7 mg, 0.193 mmol) were combined with naphthalene (4 g) in a Schlenk flask. The flask was set in a preheated sand bath (250 °C) and stirred for 12 h during which the reaction mixture turned brown. After cooling to room temperature the reaction mixture was washed with hot hexanes (2 × 40 mL). The residual brown solid was then extracted with dichloromethane (50 mL), reduced to 20 mL in vacuo, and layered with hexanes (40 mL). X-ray quality crystals of **1** were obtained after 3 days. Yield: 77.9 mg, 21.8%. Anal. Calcd for $Mo_2RuCl_2C_{40}H_{32}N_{12}$: C 45.99, H 3.09, N 16.09. Found: C 45.00, H 2.97, N 15.37. ^{1}H NMR (CD_2Cl_2, 500 MHz, ppm): δ 9.22 (4H, d, J = 6.16 Hz), 9.21 (4H, d, J = 5.73 Hz), 7.25 (4H, t, J = 7.89 Hz), 7.19 (4H, t, J = 7.51 Hz), 7.15 (4H, d, J = 8.25 Hz), 7.01 (4H, d, J = 8.50 Hz), 6.52 (4H, t, J = 6.68 Hz), 6.50 (4H, d, J = 6.70 Hz). ^{13}C NMR (CD_2Cl_2, 125 MHz, ppm): δ 166.9, 163.5, 156.62, 150.72, 135.46, 134.98, 114.07, 113.53, 112.37, 110.94. IR (ATR, cm^{-1}): 3073 w, 1601 w, 1591 w, 1459 s, 1417 s, 1352 m, 1310 m, 1283 w, 1260 w, 1153 m, 1022 m, 1014 w, 879 w, 855 w, 759 s, 740 s, 670 w.

*$[MoMoRu(dpa)_4Cl_2][SO_3CF_3]$ (**2**).* Crystalline $Mo_2Ru(dpa)_4Cl_2$ (199 mg, 0.190 mmol) was dissolved in 10 mL of CH_2Cl_2, and blue $FeCp_2(SO_3CF_3)$ (81 mg, 0.24 mmol) was dissolved in 20 mL of CH_2Cl_2. The blue $FeCp_2(SO_3CF_3)$ solution was slowly added to the brown/red $Mo_2Ru(dpa)_4Cl_2$ solution upon which a color change to purple occurred. The reaction mixture was stirred for 1 h, and then the solvent was removed under vacuum. The remaining solid was washed with diethyl ether (2 × 50 mL), discarding the orange filtrate and leaving behind a brown solid. The remaining solid was extracted with 40 mL of CH_2Cl_2. X-ray quality crystals, with the same unit cell, were grown by the slow diffusion of hexane (60 mL) or diethyl ether (60 mL) into the CH_2Cl_2 solution. Yield: 195 mg, 85.9%. Anal. Calcd for $Mo_2RuC_{41}H_{32}N_{12}Cl_2SO_3F_3$: C, 41.25; H, 2.70; N, 14.08. Found: C, 40.68; H, 2.70; N, 13.59. IR (ATR, cm^{-1}): 3012 w, 1949 w, 1654 m, 1603 m, 1550 w, 1470 m, 1458 s, 1423 s, 1343 m, 1310 m, 1281 m, 1258 m, 1236 m, 1158 m 1123 w, 1058 w, 1030 m, 858 m, 764 s, 750 s, 743 m, 692 w, 668 w, 636 s.

ASSOCIATED CONTENT

Supporting Information

Additional structural and orbital figures, Cartesian coordinates, and crystallographic data (CIF). The Supporting Information is available free of charge on the ACS Publications website at DOI: 10.1021/acs.inorgchem.5b01370.

AUTHOR INFORMATION

Corresponding Author

*E-mail: berry@chem.wisc.edu.

Notes

The authors declare no competing financial interest.

ACKNOWLEDGMENTS

We thank the National Science Foundation for support under Grant CHE-1300464. DFT calculations were supported by the National Science Foundation under Grant CHE-0840494.

REFERENCES

(1) Ritleng, V.; Chetcuti, M. J. *Chem. Rev.* **2007**, *107*, 797−858.
(2) Thomas, C. M. *Comments Inorg. Chem.* **2011**, *32*, 14−38.
(3) Cooper, B. G.; Napoline, J. W.; Thomas, C. M. *Catal. Rev.: Sci. Eng.* **2012**, *54*, 1−40.
(4) Clouston, L. J.; Siedschlag, R. B.; Rudd, P. A.; Planas, N.; Hu, S.; Miller, A. D.; Gagliardi, L.; Lu, C. C. *J. Am. Chem. Soc.* **2013**, *135*, 13142−13148.
(5) Kuppuswamy, S.; Powers, T. M.; Krogman, J. P.; Bezpalko, M. W.; Foxman, B. M.; Thomas, C. M. *Chem. Sci.* **2013**, *4*, 3557−3565.
(6) Buchwalter, P.; Rosé, J.; Braunstein, P. *Chem. Rev.* **2015**, *115*, 28−126.
(7) Berry, J. F. In *Metal-Metal Bonding*; Parkin, G., Ed.; Springer: Berlin, 2010; Vol. *136*, pp 1−28.
(8) Hua, S.-A.; Cheng, M.-C.; Chen, C.-h.; Peng, S.-M. *Eur. J. Inorg. Chem.* **2015**, *2015*, 2510−2523.
(9) Nippe, M.; Timmer, G. H.; Berry, J. F. *Chem. Commun.* **2009**, 4357−4359.
(10) Cheng, M.-C.; Mai, C.-L.; Yeh, C.-Y.; Lee, G.-H.; Peng, S.-M. *Chem. Commun.* **2013**, *49*, 7938−7940.
(11) Nippe, M.; Berry, J. F. *J. Am. Chem. Soc.* **2007**, *129*, 12684−12685.
(12) Nippe, M.; Victor, E.; Berry, J. F. *Eur. J. Inorg. Chem.* **2008**, *2008*, 5569−5572.
(13) Nippe, M.; Wang, J.; Bill, E.; Hope, H.; Dalal, N. S.; Berry, J. F. *J. Am. Chem. Soc.* **2010**, *132*, 14261−14272.
(14) Nippe, M.; Bill, E.; Berry, J. F. *Inorg. Chem.* **2011**, *50*, 7650−7661.

DOI: 10.1021/acs.inorgchem.5b01370
Inorg. Chem. 2015, 54, 7660−7665

(15) Nippe, M.; Turov, Y.; Berry, J. F. *Inorg. Chem.* **2011**, *50*, 10592−10599.
(16) Turov, Y.; Berry, J. F. *Dalton Trans.* **2012**, *41*, 8153−8161.
(17) Peng et al. have reported the synthesis of an oxidized $M_A-M_B-M_C$ chain compound, $[RhCoNi(dpa)_4Cl_2][PF_6]$, see ref 10.
(18) Brogden, D. W.; Turov, Y.; Nippe, M.; Li Manni, G.; Hillard, E. A.; Clérac, R.; Gagliardi, L.; Berry, J. F. *Inorg. Chem.* **2014**, *53*, 4777−4790.
(19) Berry, J. F.; Cotton, F. A.; Murillo, C. A.; Chan, Z.-K.; Yeh, C.-W.; Chen, J.-D. In *Inorganic Syntheses*; John Wiley & Sons, Inc.: New York, 2014; Vol. *36*, pp 102−110.
(20) Sheu, J.-T.; Lin, C.-C.; Chao, I.; Wang, C.-C.; Peng, S.-M. *Chem. Commun.* **1996**, 315−316.
(21) Kuo, C.-K.; Liu, I. P.-C.; Yeh, C.-Y.; Chou, C.-H.; Tsao, T.-B.; Lee, G.-H.; Peng, S.-M. *Chem. - Eur. J.* **2007**, *13*, 1442−1451.
(22) Huang, G.-C.; Liu, I. P.-C.; Kuo, J.-H.; Huang, Y.-L.; Yeh, C.-Y.; Lee, G.-H.; Peng, S.-M. *Dalton Trans.* **2009**, 2623−2629.
(23) Berry, J. F.; Cotton, F. A.; Murillo, C. A. *Inorg. Chim. Acta* **2004**, *357*, 3847−3853.
(24) Nippe, M.; Victor, E.; Berry, J. F. *Inorg. Chem.* **2009**, *48*, 11889−11895.
(25) Bailey, P. J.; Bone, S. F.; Mitchell, L. A.; Parsons, S.; Taylor, K. J.; Yellowlees, L. J. *Inorg. Chem.* **1997**, *36*, 867−871.
(26) Bailey, P. J.; Bone, S. F.; Mitchell, L. A.; Parsons, S.; Taylor, K. J.; Yellowlees, L. J. *Inorg. Chem.* **1997**, *36*, 5420−5420.
(27) Cotton, F. A.; Daniels, L. M.; Hillard, E. A.; Murillo, C. A. *Inorg. Chem.* **2002**, *41*, 1639−1644.
(28) Chisholm, M. H.; D'Acchioli, J. S.; Pate, B. D.; Patmore, N. J.; Dalal, N. S.; Zipse, D. J. *Inorg. Chem.* **2005**, *44*, 1061−1067.
(29) Cotton, F. A.; Daniels, L. M.; Murillo, C. A.; Timmons, D. J.; Wilkinson, C. C. *J. Am. Chem. Soc.* **2002**, *124*, 9249−9256.
(30) Cotton, F. A.; Pedersen, E. *Inorg. Chem.* **1975**, *14*, 399−400.
(31) Kiehl, P.; Rohmer, M.-M.; Bénard, M. *Inorg. Chem.* **2004**, *43*, 3151−3158.
(32) Collman, J. P.; Arnold, H. J.; Weissman, K. J.; Burton, J. M. *J. Am. Chem. Soc.* **1994**, *116*, 9761−9762.
(33) Collman, J. P.; Harford, S. T.; Maldivi, P.; Marchon, J.-C. *J. Am. Chem. Soc.* **1998**, *120*, 7999−8000.
(34) Bailey, B. C.; Basuli, F.; Huffman, J. C.; Mindiola, D. J. *Organometallics* **2006**, *25*, 2725−2728.
(35) Bruker-AXS: Madison, Wisconsin, 2009.
(36) Dolomanov, O. V.; Bourhis, L. J.; Gildea, R. J.; Howard, J. A. K.; Puschmann, H. *J. Appl. Crystallogr.* **2009**, *42*, 339−341.
(37) Neese, F. *WIREs Comput. Mol. Sci.* **2012**, *2*, 73−78.
(38) Perdew, J. P. *Phys. Rev. B: Condens. Matter Mater. Phys.* **1986**, *33*, 8822−8824.
(39) Becke, A. D. *Phys. Rev. A: At., Mol., Opt. Phys.* **1988**, *38*, 3098−3100.
(40) Neese, F. *J. Comput. Chem.* **2003**, *24*, 1740−1747.
(41) Schäfer, A.; Horn, H.; Ahlrichs, R. *J. Chem. Phys.* **1992**, *97*, 2571−2577.
(42) Eichkorn, K.; Treutler, O.; Öhm, H.; Häser, M.; Ahlrichs, R. *Chem. Phys. Lett.* **1995**, *240*, 283−290.
(43) Eichkorn, K.; Weigend, F.; Treutler, O.; Ahlrichs, R. *Theor. Chem. Acc.* **1997**, *97*, 119−124.
(44) Weigend, F.; Ahlrichs, R. *Phys. Chem. Chem. Phys.* **2005**, *7*, 3297−3305.
(45) Pantazis, D. A.; Chen, X.-Y.; Landis, C. R.; Neese, F. *J. Chem. Theory Comput.* **2008**, *4*, 908−919.
(46) Löwdin, P. O. *J. Chem. Phys.* **1950**, *18*, 365−375.
(47) Löwdin, P.-O. In *Advances in Quantum Chemistry*; Per-Olov, L., Ed.; Academic Press: New York, 1970; Vol. *5*, pp 185−199.
(48) Bruhn, G.; Davidson, E. R.; Mayer, I.; Clark, A. E. *Int. J. Quantum Chem.* **2006**, *106*, 2065−2072.
(49) Pettersen, E. F.; Goddard, T. D.; Huang, C. C.; Couch, G. S.; Greenblatt, D. M.; Meng, E. C.; Ferrin, T. E. *J. Comput. Chem.* **2004**, *25*, 1605−1612.

DOI: 10.1021/acs.inorgchem.5b01370
Inorg. Chem. 2015, 54, 7660−7665